COMPARISON OF HYDROGEN PEROXIDE QUENCHING WITH ACTIVATED CARBON AND MINERAL CATALYSTS

by

Justine Elizabeth Gleason

A thesis submitted to the faculty of
The University of North Carolina at Charlotte
in partial fulfillment of the requirements
for the degree of Master of Science in
Engineering

Charlotte

2016

Approved by:

_____
Dr. Olya Keen

_____
Dr. James Amburgey

_____
Dr. Milind Khire

ABSTRACT

JUSTINE ELIZABETH GLEASON. Comparison of hydrogen peroxide quenching with activated carbon and mineral catalysts.
(DR. OLYA KEEN)

Advanced oxidation is an advanced water treatment process used for treating impaired drinking water sources, among other applications. Commonly, hydrogen peroxide (H_2O_2) is used with ultraviolet (UV) light to create hydroxyl radicals that oxidize organic matter. Due to the low molar absorptivity of H_2O_2, not all of it gets used for oxidation and residual H_2O_2 will remain after treatment. When advanced oxidation is used for drinking water treatment, residual chlorine is required for distribution purposes. Any residual H_2O_2 is oxidized by free chlorine and ultimately more chlorine is needed to achieve a target chlorine residual concentration. In order to create a more efficient chlorine residual addition, the residual H_2O_2 is removed prior to disinfection. Highly porous granular activated carbon (GAC) is commonly used as a catalyst to quench the H_2O_2 residual. The pores can be fouled over time by organic matter and surface can be oxidized by the H_2O_2 that is present in the water, and therefore GAC must be reactivated periodically increasing overall cost of water treatment. This study explored other alternatives for quenching the H_2O_2 residual, specifically mineral catalysts that would not be as susceptible to fouling by organic matter. Reaction rates for several mineral catalysts were evaluated in batch experiments and normalized to the mass and surface area of the catalyst. The catalysts performed during batch tests in the order of GAC>activated alumina> aluminum oxide>iron (III) oxide> titanium oxide> zinc >magnesium oxide.

Column testing was performed with the most feasible mineral catalysts based on rate of H_2O_2 decomposition and applicability to full-scale processes, and compared to GAC. Further column testing was done with the most promising catalysts aluminum oxide and iron (III) oxide. Through column optimization, the aluminum oxide catalyst was able to successfully lower initial H_2O_2 concentrations from 10 mg/L to 2.2 ± .3 mg/L at a 60 minute empty bed contact time (EBCT), time the solution is exposed to the catalyst, for 2.5 hour run time. Past the 2.5 hour run time, the hydroscopic nature of aluminum oxide caused a decrease in catalytic activity due to exposure to aqueous H_2O_2 solutions which was further confirmed through batch testing. Column testing with iron (III) oxide confirmed it to be an effective inorganic catalyst in quenching 10 mg/L H_2O_2 influent to 0.070 ± 0.004 mg/L effluent concentration at a 2.5 minute EBCT, proving it to be a viable alternative to GAC.

DEDICATION

To: Juan-Carlos, Mom, Dad, Jessie, and Xueying for all of your support.

ACKNOWLEDGMENTS

I would like to thank Dr. Olya Keen, my advisor, who helped guide me through the research and for giving me the opportunity to travel to Vancouver, BC to present this work. The funding for travel was provided via the UNC Charlotte Department of Civil and Environmental Engineering new faculty start-up fund. I would also like to thank the UNC Charlotte Office of Technology Transfer prototyping grant (Provisional Patent No. 160,266) which was used to fund this project.

TABLE OF CONTENTS

LIST OF ABBREVIATIONS

AOP	Advanced oxidation processes
GAC	Granular activated carbon
$HO^{\cdot}$	Hydroxyl radical
NOM	Natural organic matter
RSSCT	Rapid small-scale column testing
TOC	Total organic carbon
UV	Ultraviolet

CHAPTER 1: BACKROUND AND LITERATURE REVIEW

Advanced oxidation is a water treatment process which commonly involves combining hydrogen peroxide (H_2O_2) and ultraviolet (UV) to create hydroxyl radicals ($HO^{\bullet}$) that react with organic contaminants in water. Hydroxyl radicals have nonspecific selectivity that allows them to react with organic molecules with different chemical structure. This property of $HO^{\bullet}$ makes advanced oxidation processes (AOPs) effective for treatment of a wide range of natural and synthetic organic contaminants. It has been shown to be highly effective in the decrease of odor and taste causing compounds as well as pharmaceutical decomposition, decolorization of dyes derived from textile manufacturing, and pesticide degradation (Andrews 1999, Shu, Chang et al. 2004, Ikehata and El-Din 2005, Christensen, Gurol et al. 2009). These synthetic organic compounds are not easily biodegradable and are found in wastewater treatment plant effluents being introduced back into natural receiving waters. The $HO^{\bullet}$ is able to effectively break the bonds of these synthetic organic compounds through oxidation making the UV/H_2O_2 processes valuable.

The process of UV/H_2O_2 unfortunately is subject to competitive UV absorbance by organic contaminants in water as well as $HO^{\bullet}$ scavenging from bicarbonate, carbonate, and H_2O_2 (Glaze, Lay et al. 1995). Due to its low molar absorptivity, large doses of H_2O_2, between 2-10 mg/L, are needed to generate the appropriate amount of

radicals for advanced oxidation to occur with only 5-10 percent of H_2O_2 consumed in the process (Watts, Hofmann et al. 2012). The presence of residual H_2O_2 can cause biological regrowth in the drinking water distribution system by providing microorganisms with an oxygen source. Although H_2O_2 is not federally regulated, biofilm generation after treatment is of concern (Kommineni 2000).

Additionally, the application of UV/H_2O_2 for drinking water treatment is commonly followed by secondary disinfection using chlorine and chloramine (Liu, Andrews et al. 2003). The secondary disinfectant is needed because UV disinfection does not maintain the water's microbial quality throughout the distribution system as required to prevent the growth of bacteria for drinking water distribution (Adedapo 2005). Chlorine reacts rapidly with H_2O_2. In order to maintain residual chlorine levels as outlined by the U.S. Environmental Protection Agency in the Surface Water Treatment Rule, larger doses of chlorine are needed to achieve the necessary chlorine residual with the presence of H_2O_2, specifically, 2.09 mg/L of free chlorine is needed per 1 mg/L of H_2O_2 (EPA 2003, Swaim, Royce et al. 2008, Keen, Dotson et al. 2013). Quenching the H_2O_2 can occur through oxidation by the free chlorine and is practiced by some utilities in North America using UV/H_2O_2 but it is expensive (Watts, Hofmann et al. 2012). Additional methods of quenching H_2O_2 were studied on the bench scale using sodium thiosulfate and sodium sulfite with stoichiometric doses to quench 1 mg/L of H_2O_2 at 9.29 mg/L and 3.7 mg/L respectively (Liu, Andrews et al. 2003). Although they have proven to be effective, it is worth noting that these reagents cannot be reused and offer a

onetime use solution to removal of residual H_2O_2 subsequently increasing the cost of AOP. Other than free chlorine, these quenching agents have not been used in drinking water AOP installations. Furthermore, overdosing sulfite or thiosulfate will result in a chlorine demand, and this can occur often due to the error associated with H_2O_2 measurements (Liu, Andrews et al. 2003). As a result, the use of a heterogeneous catalyst is worth exploring from a reusability prospective.

Granular activated carbon (GAC) has been studied as a useful quenching agent and has been recommended for removal of residual H_2O_2 in current water treatment facilities (Hofman-Caris and Beerendonk 2011). Its granular structure allows it to be used in fixed bed reactors. The activated carbon has a high surface area due to its porous structure and concentrated amounts of oxygen, sulfate, nitrogen, and unsaturated carbon at the surface that allow for its high adsorption capabilities. Its heterogeneous and large surface area lends itself to catalytic applicability in H_2O_2 reduction. The ability for the GAC to successfully quench residual H_2O_2 depends on H_2O_2 concentration, pH, temperature, porosity of carbon, and chemical properties of the surface area (Bach and Semiat 2011). The chemical properties at the surface of activated carbon can be modified through choice of precursor, synthesis protocol, and through post treatment. Surfaces can be made more acidic, basic, polar, or neutral (Barkauskas and Dervinyte 2004).

The decomposition of H_2O_2 using GAC involves the exchange of a hydroxyl oxygen group and a hydrogen peroxide anion producing a carbon surface with an increased oxidation potential, which will result in another H_2O_2 molecule decomposition ultimately yielding oxygen gas, water, and a regenerated carbon surface (Khalil, Girgis et

al. 2001). However, studies have shown that the repeated H_2O_2 oxidation of GAC changes the surface area and pore structure as a result of the chain reaction of the hydroxyl radical formation, causing a decrease in reaction rate and its catalytic activity (Bach and Semiat 2011). It is also worth noting that the presence of dissolved organic matter (DOM) found naturally in water saturates the surface and blocks the pores of the GAC over time prompting it to be regenerated periodically, which leads to a high operation cost. An example of decreased rate of reaction is shown in a study done at the University of Toronto where the effects on GAC kinetics of H_2O_2 decomposition was studied at the bench-scale (Li, 2013). GAC was exposed to natural organic matter (NOM) as well as H_2O_2 through different bed volumes. Analysis of the surface of the GAC showed an increase of oxygen and nitrogen groups presumed to be from the NOM saturation. The author explains initial decrease in rate of reaction in batch reactors to the NOM exposure but results show the decrease in rate of reaction would stop as exposure to bed volumes increased. The study showed that during the pilot column testing, the presence of H_2O_2 in solution had a greater effect on the decomposition kinetics than during batch reactions. The author suggests that the GAC in the column testing was exposed to dissolved oxygen from the quenching reaction of H_2O_2 whereas in the batch reactor oxygen can easily escape (Li 2013).

GAC samples from the contactors at the Lorne Park Water Treatment Facility were examined in another study and results showed that the bottom layers of GAC were less reactive than the top layer. The water in the bottom layers contained 32% more dissolved oxygen than the top layer, presumed to be the byproduct of quenched H_2O_2

from the top layers washing down and increasing ageing in the bottom layers and affecting the rate of H_2O_2 decomposition (Li 2013).

Activated carbon can accumulate biofilm biomass rapidly and subsequently reach a steady-state biofilm concentration (Velten, Boller et al. 2011). This can lead to plugging resulting in more frequent backwashing, which would only partially return to its original hydraulic performance (Gibert, Lefèvre et al. 2013). Regeneration of GAC would typically require thermal treatment without complete restoration to virgin state. A study reported by the Drinking Water Agency of the Municipal Environmental Research estimated a 6% loss of carbon per thermal reactivation cycle that occurs, depending on the type of water, about every 2.4 months (Culp 1981). This regeneration is only common when large quantities are used (Crittenden, Trussell et al. 2012). Biofilm growth and DOM adsorption could potentially affect catalytic activity of GAC as a result of clogging pores in the GAC. In contrast, inorganic surfaces do not provide a carbon source for bacterial growth nor exhibit considerable DOM adsorption like that of GAC. Removal of any biomass growth would occur from backwashing and sloughing off the attached growth.

In 2004, a full-scale UV/H_2O_2 treatment system was installed in the Andijk water treatment plant in the Netherlands and residual H_2O_2 concentrations were removed via GAC. The GAC filters were able to lower 6 mg/L of H_2O_2 for more than two years (Kruithof, Kamp et al. 2007). In the United States, there is the Aurora Reservoir Water Purification Facility in Colorado, which also uses GAC for the removal of residual H_2O_2 and assimilable organic carbon, a readily bioavailable fraction of DOM that increases

during the UV/H_2O_2 process. A treatment plant at Cornwall in Ontario Canada uses the UV/H_2O_2 process in order to control taste and odor compounds in the influent. This plant does not have a GAC filter but instead quenches residual H_2O_2 with chlorine. When switching between UV and UV/H_2O_2 the chlorine needs to be adjusted downstream for quenching of residual H_2O_2 to obtain a consistent goal of a regulated residual chlorine level of 0.5 mg/L (Pantin 2009).

To combat the high costs associated with managing GAC through reactivation after fouling, this study tested aluminum oxide, zinc, silver, magnesium oxide, activated alumina, titanium, titanium oxide, and iron (III) oxide for their ability to catalytically quench residual H_2O_2, and their effectiveness was compared to GAC.

These catalysts were chosen based on a comprehensive review by Garwig (1966) which summarized the effectiveness of a variety of inorganic heterogeneous catalysts to decompose H_2O_2 to be used in air propulsion systems. These systems use up to 98 percent H_2O_2 for rocket applications which means that the reviewed catalysts exhibited active and stable traits in the decomposition of high strength H_2O_2. In that report, background information was provided on a variety of inorganic catalysts. Catalysts were grouped by their purities and a variety of those with impurities and oxides were listed along with their ability for catalytic decomposition of H_2O_2. For this study, several catalysts were chosen from those identified by Garwig (1966) for further investigation. It was important that the catalysts exhibit characteristics that would allow for their use in water treatment on a large scale in fixed bed reactors. The size of the granule was taken into account in that the powdered and small granule catalysts would be hard to contain in

a fixed bed column and would require excessive pumping. One of the critical factors in selecting catalysts was low solubility to prevent leaching that could violate EPA drinking water standards. The final selection of iron (III) oxide, aluminum oxide, zinc, silver, magnesium oxide, titanium, and titanium oxide were ultimately based on these factors and the catalyst's commercial availability.

CHAPTER 2: MATERIALS AND METHODS

2.1 Reagents

Reagent grade H_2O_2 solution (30%), potassium iodide, sodium hydroxide, potassium phthalate monobasic, and ammonium molybdate tetrahydrate was obtained from Sigma-Aldrich (St. Louis, MO). All solutions were diluted using ultrapure water obtained from an Easypure II UV/UF Barnstead Thermolyne Model number D8611 (ThermoFischer, Pittsburg, PA).

2.2 Catalysts

Table 1: Catalysts used in the study

Catalyst	Chemical Formula	Vendor	CAS #	Granular Size	Water Solubility*
Activated Alumina	Al_2O_3	Purewatersite (Sandpoint, ID)	1333-84-2	3.2 mm	Insoluble in water (Sigma-Aldrich 2015)
Aluminum Oxide	Al_2O_3	Sigma-Aldrich (St. Louis, MO)	1344-28-1	3mm	Insoluble in water (Sigma-Aldrich 2015)
GAC –DSRA	C	Calgon Corporation (Pittsburg, PA)	7440-44-000	Sieved	Carbon component insoluble in water (Calgon Carbon 2013)
Iron (III) Oxide	Fe(OH)O	Sigma-Aldrich (St. Louis, MO)	20344-49-4	0.3-0.6mm	Insoluble in water (Acros Organics, 2006)
Magnesium Oxide	MgO	Sigma-Aldrich (St. Louis, MO)	1309-48-4	0.3-2mm	Insoluble in water (Sigma-Aldrich 2015)
Silver	Ag	Art-Beads (Gig Harbor, Washington)	7440-22-4	2mm	Insoluble in water (Teckcominco 2003)
Titanium	Ti	Sigma-Aldrich (St. Louis, MO)	7440-32-6	5-10mm	Insoluble in water (Sigma-Aldrich 2014)
Titanium dioxide	TiO_2	Kurt Leseker (Jefferson Hills ,PA)	13463-67-7	3-6mm	Insoluble in water (KurtLesker 2012)
Zinc	Zn	Sigma-Aldrich	7440-66-6	6mm	Insoluble in water (Avantor, 2009)

*Insoluble if greater than 10,000 mL of solvent is needed to dissolve 1 g of solute (Sigma-Aldrich 2016).

2.3 Triiodide Method

During timed reactions H_2O_2 concentrations were measured using an adapted spectrophotometric triiodide method (Klassen, 1994). This method is based on the following reactions A and B.

$$H_2O_2 + 2I^- + 2H^+ \rightarrow I_2 + H_2O \qquad (A)$$

$$I_2 + I^- \leftrightarrow I_3^- \qquad (B)$$

When large concentrations of potassium iodide are present, reaction B equilibrium is pushed to the right towards triiodide. Since triiodide absorbs light at 351 nm and is directly correlated to the amount of H_2O_2 present in the solution, H_2O_2 is measured spectrophotometrically. The relationship between absorbance and concentration is shown in equation 1, known as Beer- Lambert Law, where A is absorbance, ϵ is the molar absorptivity, c is concentration, and b is the path length of the light.

$$A = \epsilon bc \qquad (1)$$

The adapted triiodide method uses 0.563 mL aliquots of reagents A and B (described below) with a 0.125 mL aliquot of sample in a cuvette with 1 cm path length to allow the reactions to occur in the cuvette alone which conserves the reagents and minimizes the generation of hazardous waste compared to the original method. The linear concentration range of the adapted method is up to 13 mg/L. Reagent A is made from 36.67 g of potassium iodide, 1.11 g of sodium hydroxide, and 0.11 g ammonium molybdate tetrahydrate diluted to 1 liter using ultrapure water, and reagent B is made from 11.11 g

of potassium phthalate monobasic diluted to 1 liter using ultrapure water. The chemical reaction A is slow and is accelerated using ammonium molybdate tetrahydrate as a catalyst present in reagent A. This method has an accuracy of H_2O_2 concentrations as low as 1μM, which is approximately 0.034 mg/L (Klassen, 1994).

2.4 Batch Reactions

Batch reactions were carried out in 100 mL amber glass jars with a tin foil lid that prevented any light getting in to avoid photocatalytic quenching of H_2O_2 as well as for ease of sampling. Batch experiments consisted of 10 grams of catalyst and 100 mL of 10 mg/L H_2O_2 initial solution as measured prior to introduction into reactor. GAC granules were sieved between 10 and 30 US standard size sieves, 0.6mm- 2.0mm, to achieve uniform size due to a large granular size distribution as purchased. The rest of the catalysts were used as purchased and the grain sizes are listed in Table 1. The catalysts were weighed to 10 grams using a SI-114 Denver Instrument analytical balance (Bohemia, NY) and placed into batch reactors. Initial 100 mL of 10 mg/L H_2O_2 solutions were prepared using ultrapure water. Measurements of the initial 10 mg/L solution was done in triplicate before introduction to the reactor. Once introduced, the tin foil lid was immediately applied. Reactions were timed and H_2O_2 concentration levels were measured every 10 minutes using the triiodide method for a minimum of 3 hours to provide consistency between experiments.

When decomposition experiments were performed, rates of reactions were considered to be first-order reactions that follow the relationship expressed in equation 2. First-order reaction rate was determined based on previous studies of H_2O_2 quenching with GAC (Bach and Semiat 2011, Rey, Zazo et al. 2011). Equation 3 was used to

calculate the mass normalized rate of reaction for each catalyst, where m is the mass of catalyst in grams, t is time in seconds, and $[H_2O_2]$ is the molar concentration of H_2O_2. Since the reaction occurs at the surface of the catalyst, surface normalized rate constants were estimated for the minerals. Since the grain shapes differed between catalysts, an assumption was made that they all were of uniformly spherical shape. Reaction rates were compared and statistically analyzed using the 2-sample Student's T-Test.

$$r_{H_2O_2} = \frac{-d[\mathrm{H}_2 O_2]}{dt} \tag{2}$$

$$r'_{H_2O_2} = \frac{-\Delta[H_2O_2]}{\Delta t}\frac{1}{m} \tag{3}$$

2.5 RSSCT Testing

Once reaction rates in batch reactors were measured, top performing catalysts were chosen for column testing based on their overall physical properties and catalytic activity. The inorganic catalysts were compared in performance to GAC in the column tests. Rapid small-scale column tests, RSSCT, were performed to gain further insight of catalytic function in continuous flow application. RSSCT was developed by Crittenden and Reddy (1991) as a small-scale column that is scaled down from a large-scale column to have similar mass transfer processes in order to save time and expenses in pilot scale testing. The basis is that, although smaller in size, the column will have the same hydraulics with just a percent of the volume and empty bed contact time (EBCT), and

thus similar results can be obtained. EBCT describes the amount of time that the activated carbon is in contact with the solution. This is done by sizing down dimensionless factors that describe adsorbate transport using a scaling factor SF, shown in equation 4. This scaling factor can then be applied to EBCT, hydraulic velocity, υ, and diameter of the column, d (Crittenden, Reddy et al. 1991). Although this method was developed to be applied for adsorption columns, this method was used in this study for both the adsorption and the catalysis columns in order to achieve similar EBCTs as would be on a larger scale commercial applications and to effectively compare outcomes. In order to continue with comparative testing with GAC, column fittings and sizing of the GAC and inorganic catalyst columns were identical as well as particle sizes. Columns were to be run simultaneously. In order to calculate the proper sizing for initial column testing, equations 4 and 5 were used and the results are shown in Table 2; where, LC stands for large column and SC stands for small-scale column, V_{bed} is bed volume in mL, and Q is flow rate in mL/min.

$$SF = \frac{d_{p,SC}}{d_{p,\mathrm{LC}}} = \frac{EBCT_{SC}}{EBCT_{LC}} = \frac{\upsilon_{i,SC}}{\upsilon_{i,LC}} \qquad (4)$$

$$EBCT = \frac{V_{bed}}{Q} \qquad (5)$$

Another important parameter is size of granule. Although catalysts were purchased in granular form, it is important to assure that the size does not cause channeling in the column and wall effect. Crittenden noted that by having a column

diameter, $D_{column,}$ to particle diameter, d_{p} , ratio greater than 50, wall effect would be avoided. This is shown in equation 6 (Crittenden, Berrigan et al. 1986).

$$50 \leq \frac{D_{column}}{d_{p,sc}} \qquad (6)$$

By applying equations 4 through 6, small-scale columns were constructed that ultimately gave further insight on catalytic function in a flow reactor and applicability of an inorganic catalysts for the quenching of residual H_2O_2.

Columns were hooked up to a VWR (Radnor, PA) mini variable flow pump for flow rates <10 mL/min and a Masterflex (Vernon Hills, IL) digital console drive pump for flow rates >10 mL/min. This allowed for flow rates to be adjusted so that they were identical in the two columns compared side by side. The columns were fitted with identical length of tubing and fittings to allow for duplicate hydraulic conditions. Using RSSCT scaling equations previously mentioned, the dimensions of the columns were calculated. In order to achieve similar granular size of catalysts, a blender was used and catalysts were sieved to achieve a fraction of 40-60 mesh, a 0.34 mm average size. SF was calculated by the ratio of diameters of the particle sizes from large to small-scale using equation 4. The particle size of the small-scale column was determined to negate wall effect shown in equation 6 for a 21 mm schedule 40 clear PVC pipe. Table 2 shows the dimensions calculated for the construction of the columns. Glass wool (Acros Organics, Geel, Belgium) and glass beads (Fisher Scientific, Pittsburg, PA) were used at

the inlets and the outlets of the columns for distribution of flow and to prevent movement of the packing material in the column.

Table 2: Column parameters of RSSCT used for comparison of GAC and aluminum oxide

	Large Column (Gary et al. 2005)*	Small Column
Internal Diameter (mm)		16
Mean Particle Size (mm)	1.2	0.34
Scaling Factor, SF		0.29
Media Depth (mm)	850	67
EBCT (min)	3	0.88
Hydraulic Loading Rate ,v (m/hr)	10	2.9

*Parameters of large column based on range suggested by adsorbent vendor.

Five liters of 10 mg/L H_2O_2 solutions were made from the 30% H_2O_2 (Sigma-Aldrich, St. Louis, MO) using tap water to create an influent that contains total organic carbon similar to conditions that the catalysts would be exposed to in large scale applications. This would increase potential fouling rates in the granular activated carbon by the presence of total organic carbon in the system giving more accurate results.

Influent was pumped through the column and effluent was drained out into the sink. Every 30 minutes small aliquots of samples were collected into a beaker and measured for H_2O_2 concentration using the triiodide method.

2.6 Additional Column Testing for Inorganic Catalysts

In order to achieve longer EBCTs additional column testing was performed. Based on results from RSSCT testing, inorganic catalyst needed longer EBCT than that

of GAC, and further experimentation focused on optimization of EBCT for inorganic catalysts. Utilizing the same theory behind RSSCT a column was constructed that would negate wall effects. A Watson Marlow (Wilmington, MA) IP55 peristaltic pump was used in order to achieve flowrates as low as 1.3 mL/min. Table 3 shows parameters used in the construction of the small-scale columns. Goal EBCT is calculated using change in concentration obtained from RSSCT testing and applying them to the plug-flow reactor constant density model for a first-order reaction shown in equation 7 to obtain a rate of reaction which can further be applied to get an optimal EBCT.

$$\frac{dC}{d\frac{V_R}{Q}} = v_i r \qquad (7)$$

where C is concentration in mg/L , V_R is reactor volume in mL, Q is the flowrate in mL/min, r is rate of reaction in (mg/L)/min, and ν_i is stoichiometric coefficient of the limiting reactant which is unitless (Crittenden 2012).

EBCT can be further varied by changing the flow rate. Effluent concentrations were measured for H_2O_2 concentration using the triiodide method.

Table 3: Small-column dimensions for additional Al_2O_3 and Fe(OH)O testing

Parameter	Al_2O_3 Column	Fe(OH)O Column
Average Granule Size (mm), dp	0.34	.45
Internal Column Diameter (cm), D	1.6	1.6
Target EBCT (min)	20	2.5
Flow rate (mL/min), Q	4	20
Bed Volume (cm^3) , V	80	50
Cross-sectional area of column (cm^2)	2	2
Bed Length (cm) , L	41	25

CHAPTER 3: RESULTS AND DISCUSSION

3.1 Batch Testing Results

The results from batch test are shown in Figure 1, and the respective rates of reaction derived from these values are shown in Tables 4 and 5.

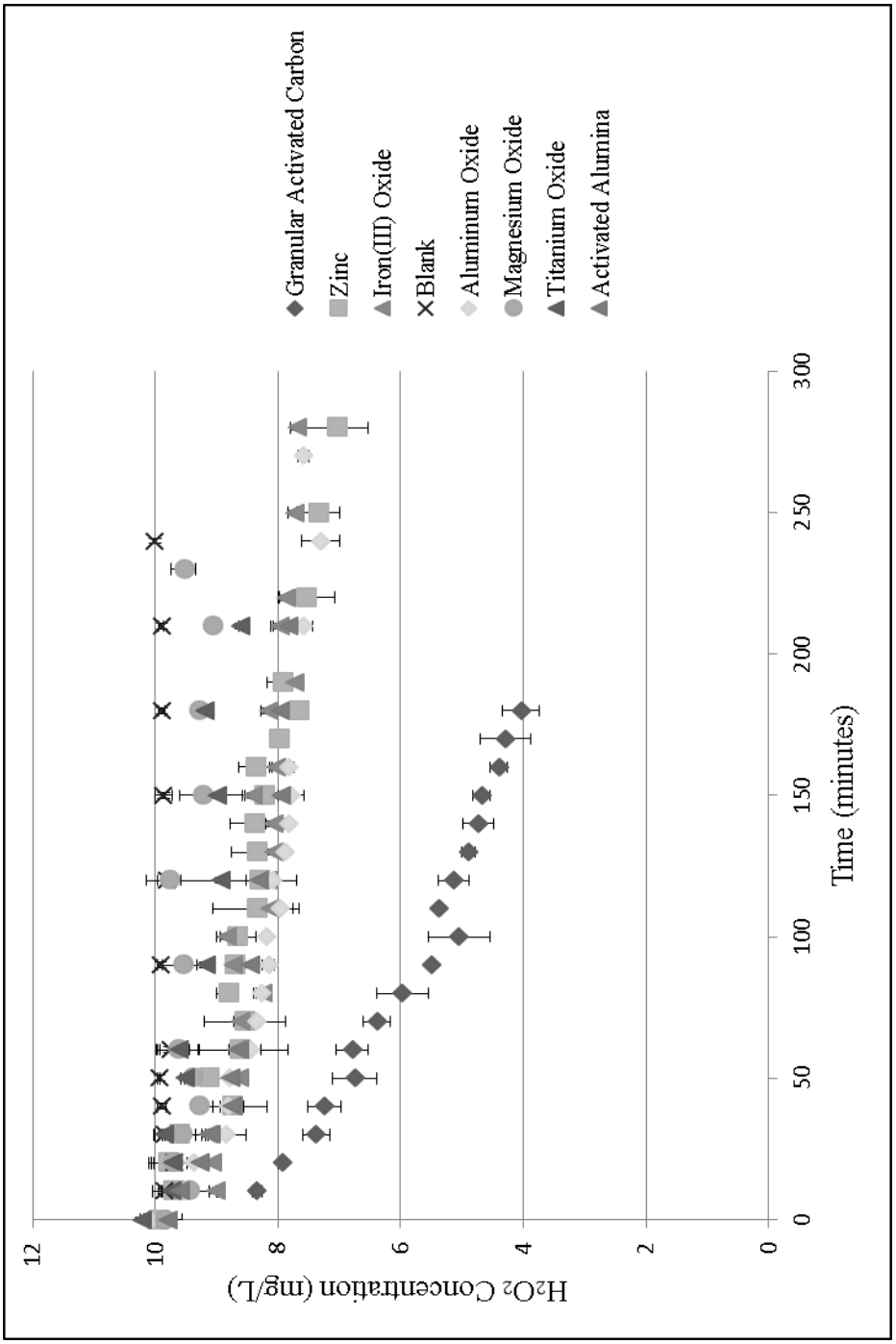

Figure 1: Batch reactor results of hydrogen peroxide decomposition

* Error Bars represent standard deviation of triplicate testing.

Table 4: Mass-normalized rates of reaction from batch experiments using

Catalyst	Rate of reaction ((moles/L)/(s·g))
GAC	$(2.1 \pm 0.6)\times10^{-9}$
Activated Alumina	$(6.9 \pm 1.3)\times10^{-10}$
Al_2O_3	$(6.9 \pm 2.6)\times10^{-10}$
Fe(OH)O	$(5.6 \pm 1.1)\times10^{-10}$
TiO_2	$(2.9 \pm 1.0)\times10^{-10}$
Zn	$(2.7 \pm 3.5)\times10^{-10}$
MgO	$(1.2 \pm 1.2)\times10^{-10}$

Table 5: Surface-area-normalized rates of reaction from batch experiment

Catalyst	Rate of reaction ((moles/L)/(s·g·mm^2)
Zn	$(2.0 \pm 2.5)\times10^{-13}$
Al_2O_3	$(1.4 \pm 0.1)\times10^{-13}$
Activated Alumina	$(3.1 \pm 0.0)\times10^{-14}$
TiO_2	$(9.3\times\pm 3.0)\times10^{-14}$
Fe(OH)O	$(1.6 \pm 0.3)\times10^{-14}$
MgO	$(7.3 \pm 7.3)\times10^{-15}$

*These results do not include GAC due to the porosity complicating surface area calculations

The results from the batch reactors showed that GAC worked the fastest followed closely by activated alumina and aluminum oxide. Silver and titanium testing showed no measurable catalytic activity (results not shown). By surface normalizing reaction rate, zinc performed the fastest with aluminum oxide pushing back to second fastest. Surface area was calculated for activated alumina not accounting for porosity and the surface normalized rate of reaction was less than that of aluminum oxide. In order to narrow down the optimal catalyst from the list for RSSCT, further tests were done in order to determine most feasible catalyst. Observations of zinc showed that although only slightly soluble, the metal was deforming to the bottom of the batch reactor causing it to stick and

therefore zinc was eliminated from any further testing as an unsuitable candidate for commercial applications in a fixed bed reactor. Titanium dioxide granules exhibited signs of breaking apart in the batch reactor and any further testing with fixed bed application was discontinued.

During testing, iron (III) oxide released insoluble particulates into the batch solution. A question arose whether it were these smaller particles that caused it to have a strong catalytic effect on the hydrogen peroxide. To test this theory, the iron (III) oxide particles were washed with ultrapure water to remove the fine particulates. Once the catalyst was washed and dried, using a 100 degree Celsius drying oven, ten grams were weighed out and batch experiments were done. Figure 2 shows the results and Table 6 compares rates of reaction. The iron (III) oxide did not show a statistically significant reduction in catalytic rate and was kept as a potential candidate for further testing.

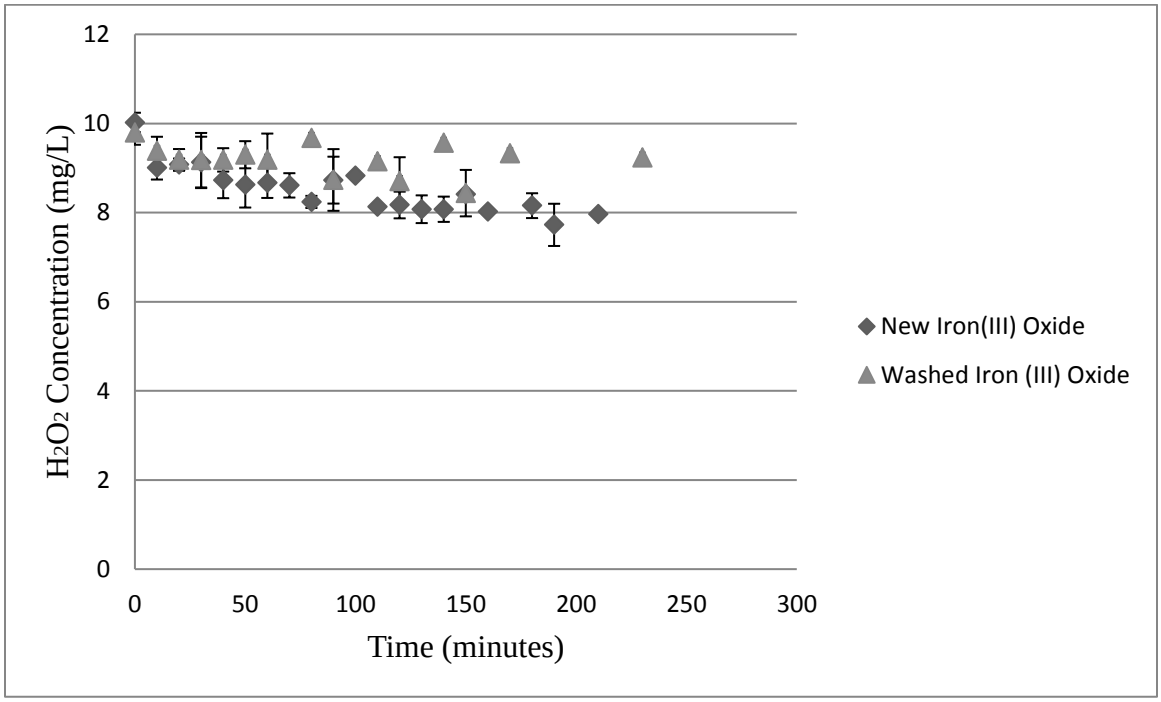

Figure 2: Comparison of New Fe(OH)O and Washed Fe(OH)O in Batch Experiment

Table 6: Reaction Rate Comparison of New and Washed Fe(OH)O

Catalyst	Rate of Reaction ((moles/L)/(s·g))
New Fe(OH)O	$(5.6 \pm 1.1)\times10^{-10}$
Washed Fe(OH)O	$(4.0 \pm 2.0)\times10^{-10}$
2- sample T-test	$\alpha = 0.05$, $p>0.05$

Similar batch experiments were run on the aluminum oxide to determine any change in catalytic rate once the catalysts were used. This is shown in Figure 3, and rate of reaction shown in Table 7.

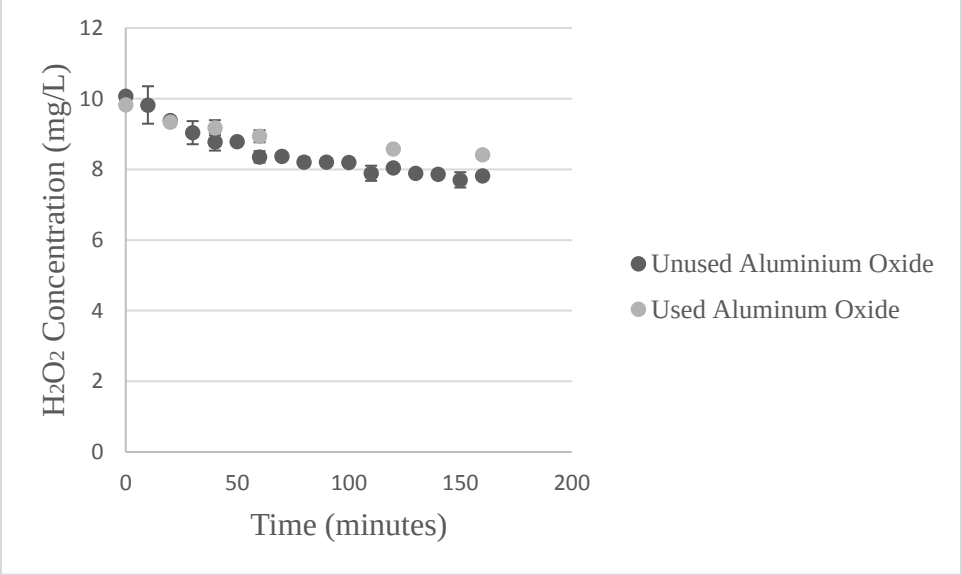

Figure 3: Comparison of unused and used Al_2O_3 batch experiments

Table 7: Comparison of unused and used Al_2O_3 rates of reaction

	Rate of reaction ((moles/L)/(s·g))
Used Al_2O_3	$(5.5 \pm 6.6)\times10^{-10}$
Unused Al_2O_3	$(6.9 \pm 2.6)\times10^{-10}$
2-sample T-test	$\alpha = 0.05$, $p>0.05$

The results showed that aluminum oxide did not lose significant catalytic strength once used, further batch testing was done to compare stirred and unstirred batch reactions. This is shown in Figure 4 and Table 8 and shows that there is no significant difference between the two batch experimental methods.

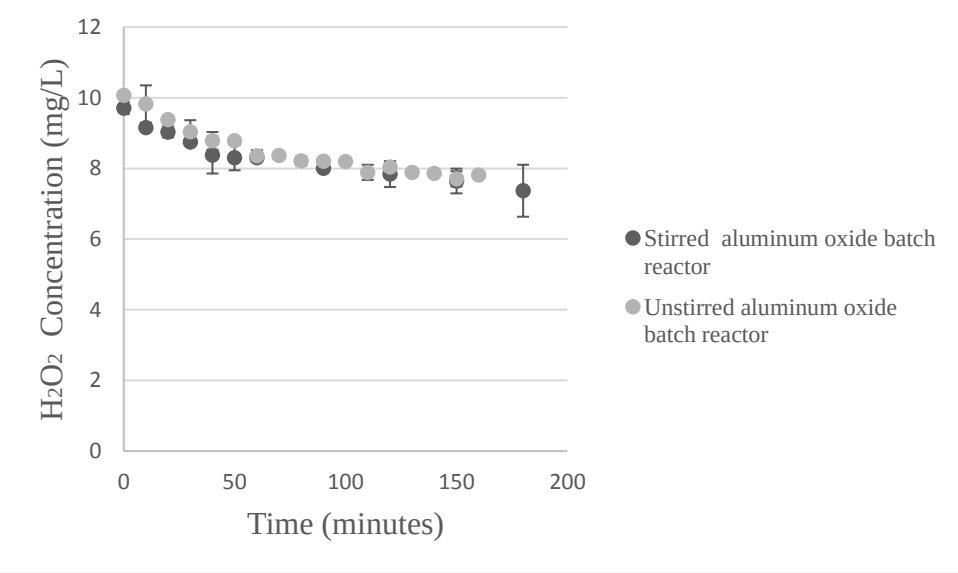

Figure 4: Stirred and unstirred Al_2O rate of reactions

Table 8: Stirred and unstirred Al_2O rate of reactions

	Rate of reaction ((moles/L)/(s· g))
Stirred Al_2O_3	$(8.4 \pm 1.1)\times10^{-10}$
Unstirred Al_2O_3	$(6.9 \pm 2.6)\times10^{-10}$
2-sample T-test	$\alpha = 0.05$, $p>0.05$

Comparative batch testing was performed between aluminum oxide and the reportedly highly porous form of aluminum oxide, activated alumina. Results are show in in Figure 4 with rates of reaction shown in table 9.

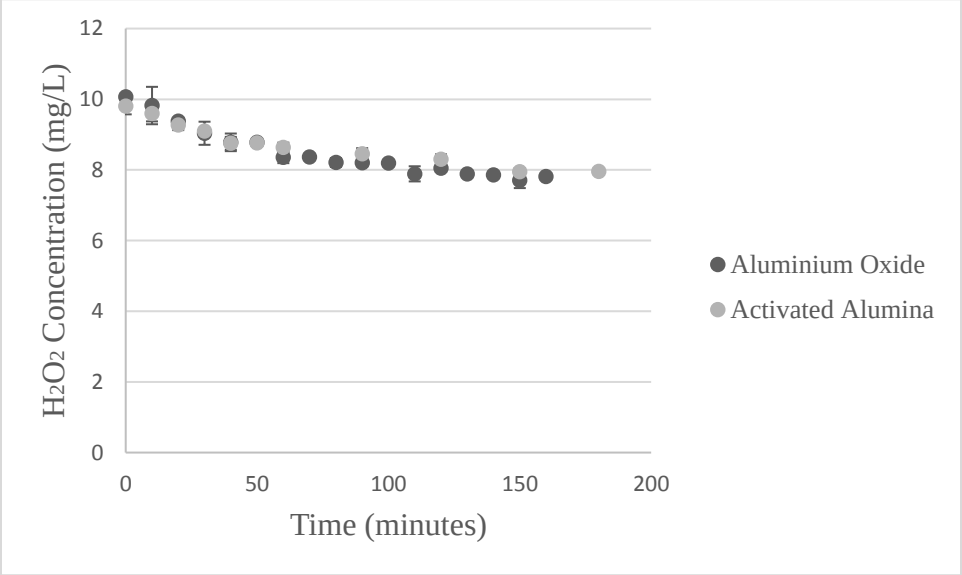

Figure 4: Comparison of Al_2O_3 and activated alumina batch experiments

Table 9: Comparison of Al_2O_3 and activated alumina rates of reaction

Catalyst	Rate of Reaction ((moles/L)/(s·g))
Al_2O_3	$(6.9 \pm 2.6)\times10^{-10}$
Activated Alumina	$(6.9 \pm 1.3)\times10^{-10}$
2-sample T-test	$\alpha = 0.05$, $p>0.05$

To further gain insight on the activated alumina, batch tests comparing used and unused were performed. Activated alumina was dried at 100 degrees Celsius before being reused because it is hygroscopic and will retain water and give inaccurate catalyst mass. The results of the comparison are shown in Figure 5 and the mass normalized rates of reaction in Table 10. No statistically significant loss of catalytic activity upon reuse was observed for any of the catalysts that were to be used in a column study.

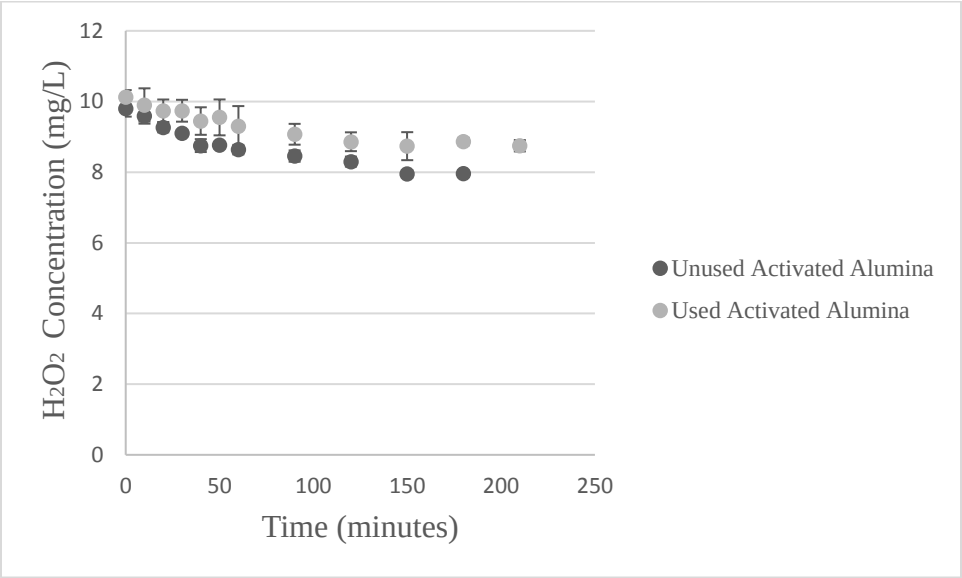

Figure 5: Comparison of unused and used activated alumina batch experiment

Table 10: Comparison of unused and used activated alumina rates of reaction

	Rate of reaction ((moles/L)/(s·g))
Used activated alumina	$(1.9 \pm 3.8)\times10^{-10}$
Unused activated alumina	$(6.9 \pm 1.3)\times10^{-10}$
2-sample T-test	$\alpha = 0.05$, $p>0.05$

Since the activated alumina did not show any significant increase in rate of reaction, the surface of the material was examined through an Olympus SZX7 (Tokyo, Japan) stereo microscope to visually compare surface of aluminum oxide with the activated alumina. Images of the surfaces are shown and compared in Figure 7 below.


(a)

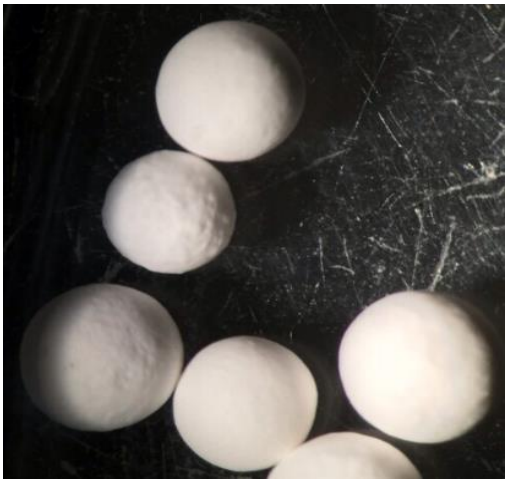
(b)

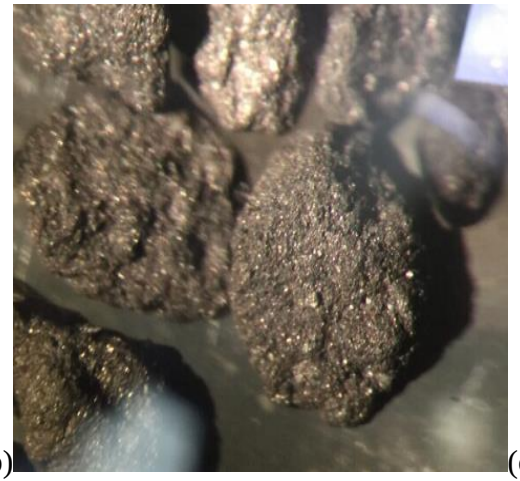
(c)

Figure 7: 100X microscope images of (a) aluminum oxide, (b) activated alumina, and (c) activated carbon surfaces

At 100 times magnification the pores and groves of the GAC were clearly visible, whereas the pores of the activated alumina were not. It was clear that statistically there was no significant difference in catalytic rate of reaction between aluminum oxide and

activated alumina and that the porous surface of activated alumina was not apparent. Due to activated alumina showing no advantages over aluminum oxide, further testing of activated alumina was deemed unnecessary.

3.2 RSSCT Testing Results

Initial H_2O_2 solutions of 10 mg/L were made from 30% reagent (Sigma-Aldrich, St. Louis, MO) and diluted with tap water. Tap water parameters and the instrument used to measure them are listed in Table 11.

Table 11: Tap water quality parameters and analyzer

Alkalinity	34.6 mg/L as $CaCO_3$	HACH Test Kit Cat #20637-00
pH	7.88	HACH-H280
Total Organic Carbon	2.75 mg/L	Shimadzu TOC-LCPN
Total Dissolved Solids	73.5 ppm	HACH-H280

The first RSSCT was performed with GAC and aluminum oxide simultaneously. H_2O_2 concentrations were measured using the adapted triiodide method. The first 125 minutes were performed with a flow rate of 20 mL/min giving effluent concentrations of 0.35 ± 0.11 mg/L for GAC and 9.42 ± 0.46 mg/L for aluminum oxide. After 125 minutes flow rates were lowered to 6 mL/min. This was done when results showed that the aluminum oxide was not working effectively. By lowering the flow rate, the EBCT was increased. The lowest flow rate the pump could output was 6 mL/min. This yielded an EBCT of approximately 4 minutes compared to 1.2 min at 20 mL/min flow rate and gave an effluent concentration of a 0.11 ± 0.05 mg/L for GAC and 7.95 ± 0.10 mg/L

for Al_2O_3 effluent concentration, shown in Figure 8. Using the SF of 0.29 outlined in Table 2, the corresponding full-scale EBCT to the RSSCT EBCTs of 1.2 minutes and 4 minutes would be 4 minutes and 14 minutes respectively.

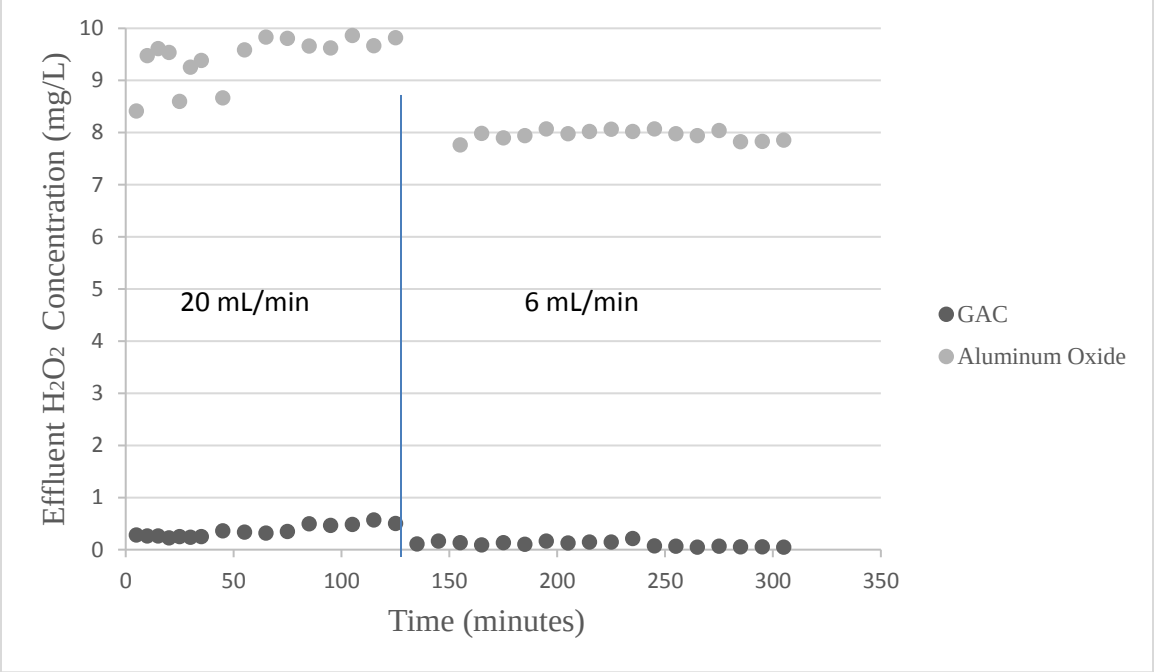

Figure 8: RSSCT results of GAC and Al_2O_3 with 10 mg/L H_2O_2 influent

3.3 Additional Column Testing for Inorganic Catalysts Results

Based on the results obtained during RSSCT it was clear that the inorganic catalyst needs longer EBCT than that of GAC to effectively quench the H_2O_2. The next phase of the research focused on establishing a column capable of longer EBCT. Optimal EBCT was calculated to be 20 minutes, the calculations are shown in Appendix A. Figure 9 shows the results from two column tests performed at 6 mL/min flow rate to achieve a 14 minute EBCT.

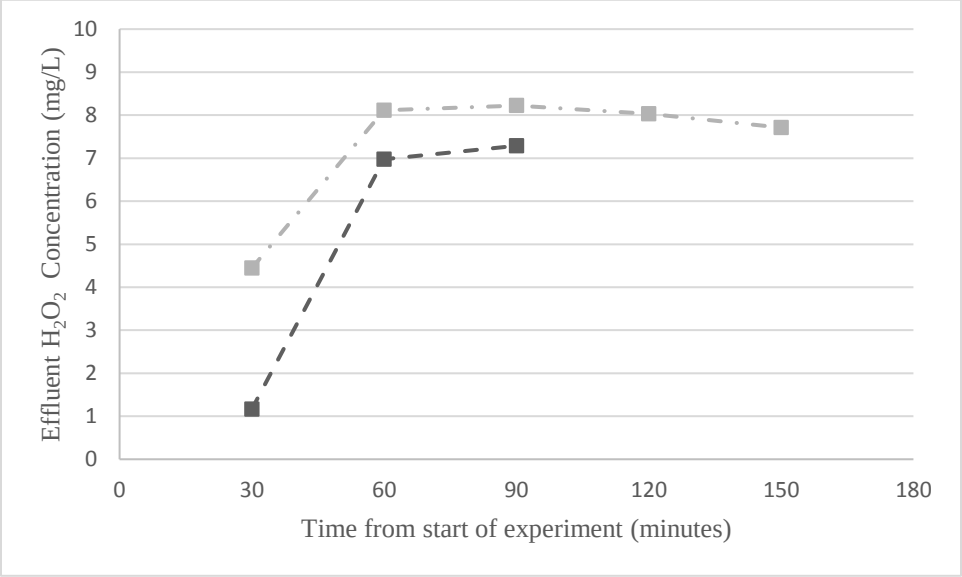

Figure 9: 6 mL/min Al_2O_3 column trial results*
*The two data sets represent the results of two trials.

Initial readings showed a 1.2 mg/L effluent reading with results sharply increasing to 7 mg/L at the 60 minute mark. A repeated experiment was performed with initial reading at 4.5 mg/L and sharp increase to 8 mg/L at the 60 minute mark where the next 2 hours resulted in 8.0 ± 0.2 mg/L readings.

In order to increase EBCT closer to the calculated 20 minute EBCT, flow rate was lowered to 1.7 mL/min for one run yielding a 50 minute EBCT, and 1.3 mL/min for two runs yielding a 60 minute EBCT. Results are shown in Figure 10.

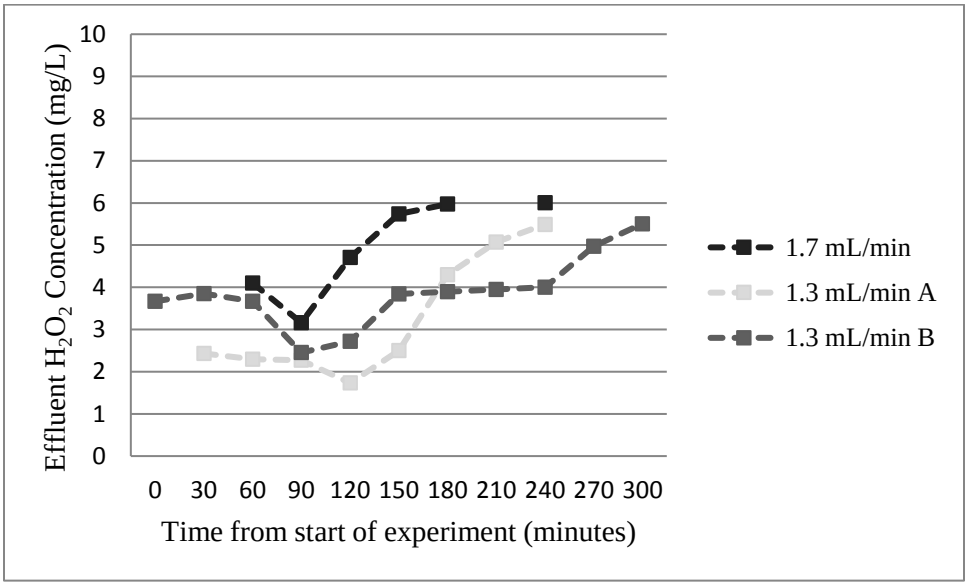

Figure 10: Additional Al_2O_3 column testing results at 1.7 mL/min and 1.3 mL/min

During the initial testing of the column at 1.3 mL/min, the effluent produced at concentrations of 2.2 mg/L ± 0.3 mg/L during the first 2.5 hours before the concentration increased demonstrating a decrease of catalytic rate. During repeats it was evident that during each run catalytic rate slowly decreased over time and that the faster was the flow rate the quicker this decrease would occur. It was hypothesized that this was due to the hygroscopic nature of aluminum oxide. It is likely that the catalyst was getting saturated with water molecules that would provide a barrier between the catalytic active sites of the surface and the H_2O_2 molecules in the solution preventing any quenching from occurring. In order to experimentally explain why this could be happening, further batch tests were completed that compared saturated aluminum oxide and unsaturated aluminum oxide.

To saturate the catalyst it was washed with ultrapure water and soaked for 1 hour, then gravity filtered through a Whatman 40 paper filter (FisherScintific, Pittsburg, PA).

Average weight percent increase due to water saturation was 55 ± 5%. Results are shown in Figure 11, with change in rate of reaction shown in Table 11.

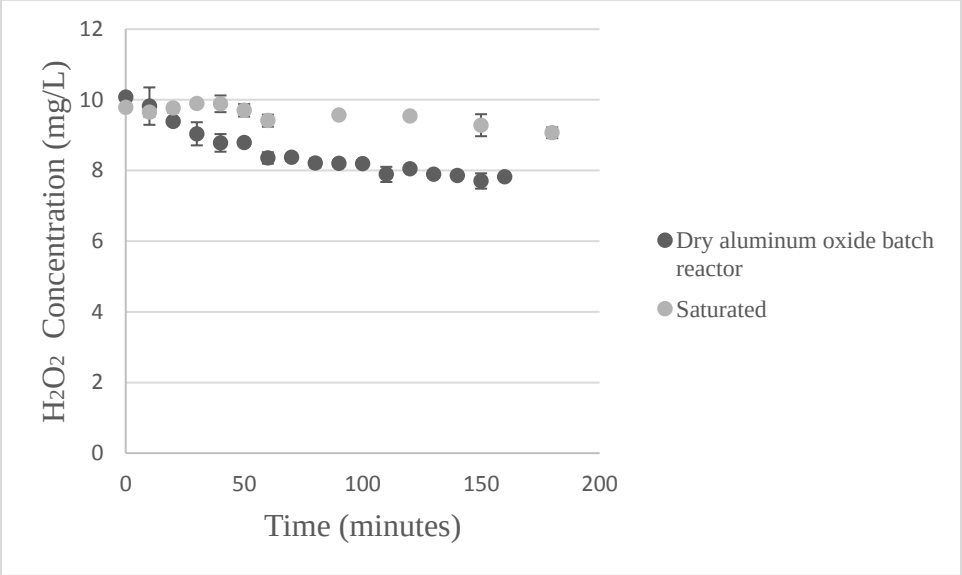

Figure 11: Saturated and dry Al_2O_3 batch reactions

Table 11: Saturated and dry Al_2O_3 rate of reactions

	Rate of reaction ((moles/L)/(s· g))
Dry Al_2O_3	$(6.9 \pm 2.6)\times10^{-10}$
Saturated Al_2O_3	$(2.4 \pm 8.9)\times10^{-11}$
2-sample T-test	$\alpha = 0.05$, $p=0.014$

Reaction rates were lowered significantly as aluminum oxide became saturated. In order to try and combat this saturation air scour was installed in the column in the attempt to add turbulence that could stave off complete saturation of the catalytic surface. Testing was completed with a 4 mL/min flowrate. Results from duplicate testing shown in Figure 12 showed that air scour did not prevent saturation of aluminum oxide catalyst.

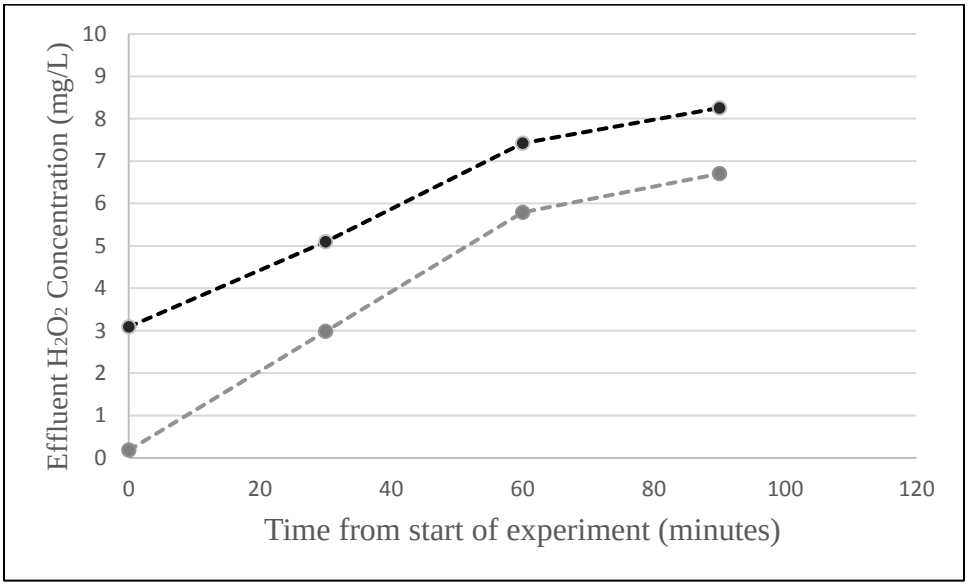

Figure 12: Duplicate Al_2O_3 air scour column results at at 4 mL/min

Further testing with Al_2O_3 was discontinued due to fast breakthrough of H_2O_2, and testing continued with iron (III) oxide whose mass–normalized rate of reaction determined in batch testing came after that of aluminum oxide and activated alumina. The iron (III) oxide catalyst was washed with tap water prior to bed packing and the column was additionally flushed with tap water after packing until all smaller particulates were removed. Unlike in the additional column testing for Al_2O_3 there were no preliminary RSSCT results to determine optimal EBCT. This was done experimentally with using 10 mg/L H_2O_2 solution and adjusting flow rate of the column. After initial 4 hours of preliminary testing which involved running the 10 mg/L H_2O_2 solution at different flow rates to determine optimal EBCT for column, the iron (III) oxide proved to be effective at all flow rates that the pump could provide, thus it was turned to its highest flow rate of 20 mL/min (2.5 min EBCT) and repeated twice. Results are shown in Figure 13 for flow rate of 20 mL/min.

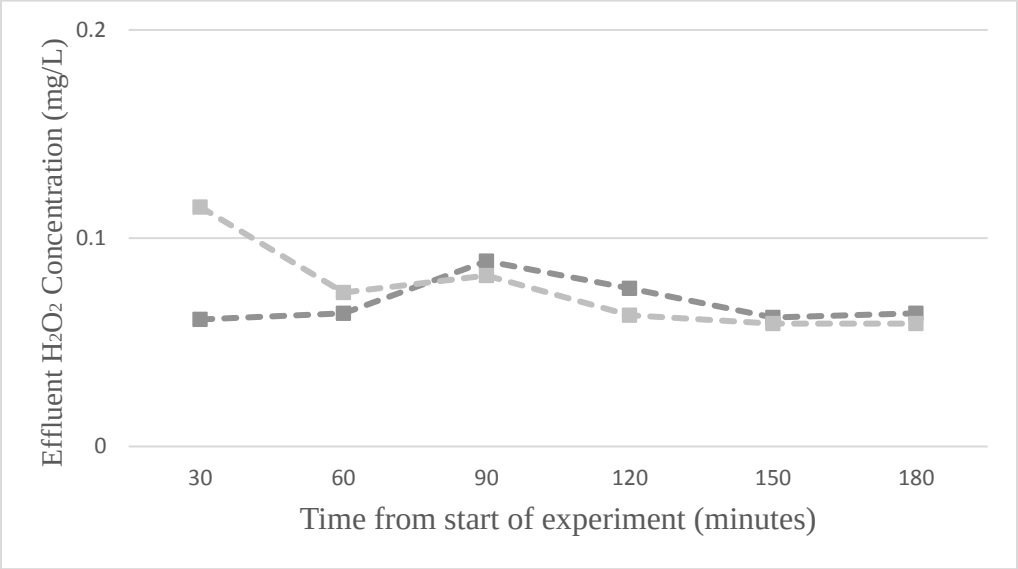

Figure 13: Column testing results of iron (III) oxide at 20 mL/min

Effluent H_2O_2 concentrations were 0.070 ± 0.004 mg/L for the iron (III) oxide column at the 2.5 minute EBCT and was sustained for the 3 hour duration of the run.

3.4 Discussion

The goal of this study was to find alternative heterogeneous catalysts to GAC to use for the quenching of residual H_2O_2 after UV/ H_2O_2 advanced oxidation process. This is because although GAC is shown to be reactive for residual H_2O_2 after treatment, studies have suggested that the surface of the GAC undergoes oxidation from H_2O_2 which changes the pore structure and decrease catalytic rate (Bach and Semiat 2011, Li 2013). Also, GAC porosity makes it susceptible to fouling caused by organic matter in the treated water and from steady state biofilm growth resulting in the need to be regenerated which increases maintenance costs (Velten, Boller et al. 2011). By using comparison studies, alternative inorganic catalysts that would not be as susceptible to fouling and biofilm growth were selected to be studied. The inorganic catalysts aluminum oxide, titanium, silver, titanium oxide, iron (III) oxide, magnesium oxide, and zinc were batch tested and results showed that aluminum oxide performed best with a reaction rate of $(6.9 \pm 2.6)\times10^{-10}$ (moles of H_2O_2/L)/(s· g). This was not as fast as the GAC batch testing which yielded a result of $(2.1 \pm 5.8)\times10^{-10}$ (moles of H_2O_2/L)/(s· g).

Another avenue that was explored was the effect porosity had on the reaction rate of the inorganic catalysts. Activated alumina, a reportedly highly porous version of aluminum oxide was explored. Results showed that the activated alumina had a reaction rate of $(6.9 \pm 1.3) \times10^{-10}$ (moles of H_2O_2/L)/(s· g) which was not significantly different than the aluminum oxide. Further inspection showed that the surface of the activated alumina was not porous as no pores were visible at 100 times magnification whereas

GAC pores were visible, and that this could be the reason why there was no significant change in rate of reaction.

Because of GAC's higher reaction rate, during RSSCT it outperformed aluminum oxide significantly. By increasing EBCT for the column, lower effluent H_2O_2 concentrations were achieved for aluminum oxide. This showed that in order to achieve significant quenching of H_2O_2 with aluminum oxide EBCT needed to be considerably higher than for GAC quenching.

Additional column testing showed that EBCT could effectively be manipulated by adjusting bed length and flowrate. Testing showed that although longer EBCT showed an increase in H_2O_2 decomposition, rate of reaction would decrease fairly quickly. A viable explanation for this would be the hygroscopic nature of aluminum oxide and that the adsorption of water molecules to the surface slows the diffusion of hydrogen peroxide molecules to the catalytic sites. This was shown through batch testing, in the saturated aluminum oxide performed significantly at a decreased rate of reaction than that of the unsaturated. Air scour did not effectively combat rapid surface saturation with water.

Attention was then focused on iron (III) oxide which had slower reaction rate than aluminum oxide and activated alumina in batch testing after with a rate of reaction of $(5.6 \pm 1.1) \times 10^{-10}$ (moles of H_2O_2/L)/(s· g). However, not being hygroscopic, the iron oxide catalyst was able to effectively quench 10 mg/L H_2O_2 influent concentrations to 0.070 ± 0.004 mg/L with a 2.5 minutes EBCT.

CHAPTER 4: CONCLUSION

The results show that the rates of reactions for the alternative catalysts for H_2O_2 quenching in batch analysis went as follows: GAC>activated alumina> aluminum oxide>iron (III) oxide> titanium oxide > zinc >magnesium oxide. In comparison to GAC, the mineral catalysts did not perform as effectively in the decomposition of the 10 mg/L H_2O_2 solution during batch testing. In the column testing, GAC performed well while the aluminum oxide column showed only a slight reaction with the same EBCT. Aluminum oxide is a hygroscopic material and the formation of water film on the surface of the granules slows down the catalytic decomposition of H_2O_2 enough to make this material not useful for the purpose on full scale. Although iron (III) oxide showed a slower rate than aluminum oxide in batch testing, column tests with EBCT of 2.5 minutes produced an effective quenching of 10 mg/L H_2O_2 concentration to 0.070 ± 0.004 mg/L. Since iron (III) oxide is non-porous and not susceptible to fouling or biofilm growth, it was proven to be a viable alternative to GAC in the use of H_2O_2 in water treatment.

Future work should focus on the side-by-side long term comparison of an iron (III) oxide column and a GAC column to compare the bed volumes treated until the H_2O_2 breakthrough for each catalyst.

REFERENCES

Acros Organics (2006, April) *Iron (III) oxide* [Safety Data Sheet] Retrieved from MSDS Online https://fscimage.fishersci.com/msds/00795.htm April 23, 2016.

Adedapo, R. Y. (2005). Disinfection By-Product Formation in Drinking Water Treated with Chlorine Following UV Photolysis & UV/H_2O_2 Civil Engineering. Waterloo, Ontario, Canada, University of Waterloo. **Master of Applied Science** 235.

Andrews, S. A., Bolton, J. R., Zheng, M. (1999). Impacts of Medium-Pressure UV and UV/H_2O_2 Treatments on Disinfection Byproduct Formation. AWWA Annual Conference. Chicago, Illinois, ResearchGate**:** 19.

Bach, A. and R. Semiat (2011). "The role of activated carbon as a catalyst in GAC/iron oxide/H2O2 oxidation process." Desalination **273**(1): 57-63.

Avantor Performance Materials (2009, April) *Zinc metal* [Safety Data Sheet] Retrieved from MSDS Online https://msdsmanagement.msdsonline.com/c3694f80-5cae-4ea6-84bd-5c5f1508ab4f/pdf/?libraryID=CWD861&pageID=1&nw=true&autoOpen=false April 23, 2016.

Bach, A. and R. Semiat (2011). "The role of activated carbon as a catalyst in GAC/iron oxide/H2O2 oxidation process." Desalination **273**(1).

Barkauskas, J. and M. Dervinyte (2004). "Investigation of the functional groups on the surface of activated carbons." Journal of the Serbian Chemical Society. **69**: 363-376.

Calgon Corportaion (2013, February) *Activated Carbon* [Safety Data Sheet] Retrieved from MSDS Online https://msdsmanagement.msdsonline.com/c3694f80-5cae-4ea6-84bd-5c5f1508ab4f/pdf/?libraryID=KLA409&pageID=1&nw=true&autoOpen=false April 23, 2016.

Christensen, A., et al. (2009). "Treatment of persistent organic compounds by integrated advanced oxidation processes and sequential batch reactor." Water Research **43**(16): 3910-3921.

Crittenden, J. C., et al. (1986). "Design of Rapid Small-Scale Adsorption Tests for a Constant Diffusivity." Journal (Water Pollution Control Federation) **58**(4): 312-319.

Crittenden, J. C., et al. (1991). "Predicting GAC Performance With Rapid Small-Scale Column Tests." jamewatworass Journal (American Water Works Association) **83**(1): 77-87.

Crittenden, J. C., et al. (2012). Adsorption. MWH's Water Treatment: Principles and Design, Third Edition, John Wiley & Sons, Inc.**:** 1117-1262.

Culp, F., Smith (1981). Granular Activated Carbon Installations. Cincinnati, Ohio, Culp/Wesner/Cupl Consulting Engineers**:** 296.

EPA (2003). LT1ESWTR Disinfection Profiling and Benchmarking. EPA Guidance Manual. O. o. Water. **2015**.

Garwig, P. L. (1966). Heterogeneous Decomposition of Hydrogen Peroxide By Inorganic Catalysts. A. F. R. P. Laboratory. Edwards, California.

Gary, A., Hsiao-wen Chen, Aleksandra Drizo, Urs von Gunten, Phil Brandhuber, Ruth Hund, Zaid Chowdhury, Sunil Kommineni, Shahnawaz Sinha, Martin Jekel, and Kashi Banerjee (2005). Adsorbent Treatment Technologies for Arsenic Removal. AWWA.

Gibert, O., et al. (2013). "Characterising biofilm development on granular activated carbon used for drinking water production." Water Research **47**(3): 1101-1110.

Glaze, W. H., et al. (1995). "Advanced Oxidation Processes. A Kinetic Model for the Oxidation of 1,2-Dibromo-3-chloropropane in Water by the Combination of Hydrogen Peroxide and UV Radiation." Industrial & Engineering Chemistry Research **34**(7): 2314-2323.

Hofman-Caris, C. and E. Beerendonk (2011). New Concepts of UV/H_2O_2 Oxidation. Water Treatment. C. a. B. Hofman-Caris, E. Nertherlands, KWR Water Research Institue**:** 293.

Ikehata, K. and M. G. El-Din (2005). "Aqueous pesticide degradation by ozonation and ozone-based advanced oxidation processes: A review (Part II)." Ozone-Science & Engineering **27**(3): 173-202.

Keen, O. S., et al. (2013). "Evaluation of Hydrogen Peroxide Chemical Quenching Agents following an Advanced Oxidation Process." Journal of Environmental Engineering **139**(1): 137-140.

Khalil, L. B., et al. (2001). "Decomposition of H₂O₂ on activated carbon obtained from olive stones." JCTB Journal of Chemical Technology & Biotechnology **76**(11): 1132-1140.

Klassen, N. V., D. Marchington and H. C. McGowan (1994). "H_2O_2 Determination by the I_3^- Method and by $KMnO_4$ Titration." Analytical Chemistry **66**(18): 2921-2925.

Kommineni, S., Zoeckler, J, Stocking, A.J; Liang, S.; Flores, A.E.; Kavanaugh, M.C. (2000). Treatment Technologies for Removal of Methyl Tertiary Butyl Ether (MTBE) from Drinking Water. N. W. R. I. Gina Melin, The California MTBE Research Partnership.

Kruithof, J. C., et al. (2007). "UV/H2O2 Treatment: A Practical Solution for Organic Contaminant Control and Primary Disinfection." OZONE SCIENCE AND ENGINEERING **29**(4): 273-280.

KurtLesker (2012, March) *Titanium dioxide* [Safety Data Sheet] Retrieved from Kurt J. Lesker Company Online

https://www.lesker.com/msds/pdfs/8d6e3931e6483f2073a7928076e412925bad26cded0dfd05adb75d76c.pdf April 23, 2016.

Li, J. (2013). Quenching H_2O_2 Residuals after UV/H_2O_2 Drinking Water Treatement Using Granular Activated Carbon. Graduate Department of Civil Engineering. Toronto, University of Toronto. **Master of Applied Science:** 141.

Liu, W., et al. (2003). "Optimal methods for quenching H2O2 residuals prior to UFC testing." Water Research Water Research **37**(15): 3697-3703.

Pantin, S. (2009). Impact of UV-H_2O_2 Treatment for Taste and Odour Control of Secondary Disinfection. Graduate Departmentof Civil Engineering. Toronto, University of Toronto. **Master of Applied Science:** 167.

Rey, A., et al. (2011). "Influence of the structural and surface characteristics of activated carbon on the catalytic decomposition of hydrogen peroxide." Applied Catalysis A: General **402**(1–2): 146-155.

R. Scott Summers, A. M. K., Detlef R.U. Knappe, Allison M. Reinert, Meredith E. Fotta, Angela J. Mastropole, Joseph Roccaro, and Christopher J. Corwin (2014). "Evaluation of Available Scale-up Approaches for the Design of GAC Contactors.". Retrieved March 26, 2016, 2016.

Shu, H.-Y., et al. (2004). "Decolorization of azo dye acid black 1 by the UV/H2O2 process and optimization of operating parameters." Journal of Hazardous Materials **113**(1–3): 201-208.

Sigma-Aldrich (2015, February) *Magnesium oxide* [Safety Data Sheet] Retrieved from Sigma-Aldrich Online http://www.sigmaaldrich.com/Graphics/COfAInfo/SigmaSAPQM/SPEC/22/220361/220361-BULK_____SIAL_____.pdf April 23, 2016.

Sigma-Aldrich (2015, March) *Aluminum oxide & activates alumina* [Saftey Data Sheet] Retrieved from MSDS Online https://msdsmanagement.msdsonline.com/c3694f80-5cae-4ea6-84bd5c5f1508ab4f/pdf/?libraryID=LPM877&pageID=1&nw=true&autoOpen=false April 23, 2016.

Sigma-Aldrich (2014, June) *Titanium* [Saftey Data Sheet] Retrieved from Sigma-Aldrich Online http://www.sigmaaldrich.com/Graphics/COfAInfo/SigmaSAPQM/SPEC/30/305812/305812-BULK_____ALDRICH__.pdf April 23, 2016.

Sigma-Aldrich (2016). "Solubility Information." Retrieved July 19, 2016, 2016, from http://www.sigmaaldrich.com/united-kingdom/technical-services/solubility.html.

Swaim, P., et al. (2008). "Effectiveness of UV Advanced Oxidation for Destruction of Micro-Pollutants." Ozone: Science & Engineering **30**(1): 34-42.

Teckcominco (2003, Decmeber) *Silver metal* [Safety Data Sheet] Retrieved from MSDS Online https://msdsmanagement.msdsonline.com/c3694f80-5cae-4ea6-84bd-5c5f1508ab4f/pdf/?libraryID=361328&pageID=1&nw=true&autoOpen=false April 23, 2016.

Velten, S., et al. (2011). "Development of biomass in a drinking water granular active carbon (GAC) filter." Water Research **45**(19): 6347-6354.

Watts, M. J., et al. (2012). "Low-pressure UV/Cl₂ for advanced oxidation of taste and odor." J Am Water Works Assoc Journal - American Water Works Association **104**(1): 47-48.

APPENDIX A: OPTIMAL EBCT CALCULATIONS

$$\frac{dC}{d\frac{V_R}{Q}} = v_i r$$

Where:

C= Cocentration (mg/L)

V_R = volume of reactor (mL)

Q = Flow rate (mL/min)

r = rate of reaction ((mg/L)/min)

v_i = stoichometric coefficient of limiting reactant (unitless)

$$\frac{10\frac{mg}{L} - 8\frac{mg}{L}}{\frac{23.8mL}{21.7\frac{mL}{\min}}} = -r$$

$$r = 0.50\frac{\frac{mg}{L}}{\min}$$

$$\frac{10\frac{mg}{L} - 0\frac{mg}{L}}{0.5\frac{\frac{mg}{L}}{\min}} = 20\min$$